Kinetics of palladium oxidation in the mbar pressure range: *Ambient Pressure XPS study*

Dmitry Zemlyanov*,[1,2] Bernhard Klötzer,[3] Harald Gabasch,[3] Andrew Smeltz,[4] Fabio H. Ribeiro,[4] Spiros Zafeiratos,[5,a] Detre Teschner,[5] Peter Schnörch,[5] Elaine Vass,[5,b] Michael Hävecker,[5] Axel Knop-Gericke,[5] Robert Schlögl[5]

[1]*Birck Nanotechnology Center, Purdue University, 1205 West State Street, West Lafayette, IN 47907-2057, USA*

[2]*Materials and Surface Science Institute, University of Limerick, Limerick, Ireland*

[3]*Institut für Physikalische Chemie, Universität Innsbruck, A-6020, Innsbruck, Austria*

[4]*School of Chemical Engineering, Purdue University, 480 Stadium Mall Drive, West Lafayette, IN 47907-2100, USA*

[5]*Abteilung Anorganische Chemie, Fritz-Haber-Institut der Max-Planck-Gesellschaft, Faradayweg 4-6, D-14195 Berlin, Germany*

Phone: +1 (765) 496-2457

Fax: +1 (765) 496-8299

Email: dzemlian@purdue.edu

URL: http://www.purdue.edu/dp/Nanotechnology/facilities/XPS.php

Present address: [a] LMSPC-UMR 7515 du CNRS; 25, rue Becquerel; F 67087 Strasbourg Cedex 2; France
[b] Johnson Matthey Catalysts, PO Box 1, Belasis Avenue, Billingham, Cleveland, TS23 1LB, UK

Abstract

Palladium oxidation was studied by ambient pressure XPS in the mbar pressure range on the Pd(111) and Pd(110) surfaces. The oxidation kinetics on both surfaces show an induction period when the oxidation rate was low at the beginning and then accelerated. The slow initial oxidation is governed by (a) the rate of nucleus formation, and by (b) the rate of oxide nucleus growth. Depth profiling varying photon energy/kinetic photoelectron energy pointed to a 3D oxidation. It is remarkable that the oxidation of Pd(110) proceeds at ~100 K lower temperatures than on Pd(111). We suggest that at the high temperature required on Pd(111) nucleation is thermodynamically controlled, and therefore, the nucleation rate decreases with temperature. On Pd(110), nucleation is predominantly kinetically controlled and thus the oxidation rate increases with temperature.

Keywords: *Ambient Pressure XPS, palladium oxidation, palladium single crystal*

1. Introduction

Palladium is a widely used catalyst for a number of hydrocarbon oxidation reactions such as total methane oxidation, partial oxidation of hydrocarbons, methanol steam reforming, water gas shift reaction, etc (see for examples Refs. [1-6] and Refs therein). In many cases, the oxidative chemistry of palladium is controlled by a certain chemical state of the surface. For instance, catalytic combustion of methane is carried out under conditions varying from low temperatures, where palladium oxide is the thermodynamically stable phase, to high temperatures, where palladium metal is the stable phase [2,3,6]. It was suggested that methane oxidation over palladium occurs with the highest rate on PdO and the reaction rate drops when the thermodynamic limit of PdO stability is exceeded (see e.g. Ref.[6] and Refs therein). On the other hand, partial oxidation of ethylene requires a reduced, carbon-doped and oxygen-depleted surface; moreover, formation of a "dissolved carbon phase" is needed for enhanced selectivity towards C1 oxygenates and CO rather than CO_2 [7]. The basic conclusion is that the chemical state of palladium determines the pathway of a chemical reaction and, therefore, the mechanism of palladium oxidation is crucially important for understanding oxidative catalysis by palladium. However, an investigation of PdO formation in well-defined conditions (single crystals, UHV, etc.) is experimentally challenging due to thermodynamics limitation. Using Warner's expression [8], one can work out that in 1 mbar O_2, the PdO/Pd transition takes place at approximately 840 K. If this expression is extrapolated to low pressures, the PdO/Pd transition at 10^{-6} mbar is estimated to occur at approximately 610 K.

In the past palladium oxidation has received its fair share of attention, however, the main research stream was focused on low oxygen pressure (< 10^{-6} mbar), which is suitable for the common surface science tools (see e.g. Refs. [9-14,1,15-25] and Refs. therein). It was found that at room temperature a (2×2) O_{ads} structure with a coverage of 0.25 ML forms on the Pd(111) surface [10]. An incommensurate two-dimensional surface oxide, Pd_5O_4, forms after

exposure of the Pd(111) surface to 5×10^{-6} mbar O_2 at 300°C as reported by Lundgren *et al.* [9]. Zheng and Altman [10] observed a similar surface structure upon exposure of Pd(111) to NO_2. Yudanov *et al.* [26] computed kinetic barriers for surface-bulk migration of C, N, and O atoms and predicted that diffusion of oxygen in the bulk becomes appreciable above 900 K. Experimentally it was found that oxygen dissolved in the bulk is suggested to form a Pd-O solid solution and desorbs above 1100 K [11-14,1]. All these investigations have resulted in detailed understanding of adsorption mechanisms and reaction pathways within thermodynamic limitation due to vacuum conditions. Thermodynamic equilibrium shifts with pressure, therefore a UHV study might be not very representative for the real world. In relation to oxide phase formation, the main challenge was to generate high oxygen surface concentration in UHV. To overcome this obstacle, some researchers have tended to used stronger oxidizer such as NO_2 [18] or atomic oxygen [21-23,25]. The other have chosen a high pressure oxygen treatment followed by *ex situ* characterization [27,28]. *Ex situ* experiments using UHV surface science methods might also lead to ambiguous results/conclusions because the catalytically active species might not survive reaction quenching by removal of the reaction gases and changing the temperature.

However, an improved understanding of the oxidation mechanism is almost impossible without bridging the pressure gap by carrying out an *in situ* investigation in the mbar range close to real catalytic combustion. *In situ* surface x-ray diffraction was used to study palladium oxidation up to 1 mbar [15-17,19,20]. Ambient-pressure photoelectron spectroscopy (APPES), which is also referred to as *in situ* X-ray Photoelectron Spectroscopy (XPS) or high-pressure XPS, was demonstrated as a new tool for surface science and nanotechnology, which allows to collect photoemission spectra in mbar pressure range [29,30]. The applications of ambient-pressure PES for palladium oxidation were reported in Refs. [31-33]. The results for Pd(111) oxidation in the mbar pressure range during a temperature-programmed experiment with both a heating and cooling cycle were reported in Refs. [32,33]. The 2D Pd_5O_4 surface oxide phase was found to act as a precursor for the bulk PdO phase. Oxygen diffusion to the metal bulk dominated at high temperatures. As a result, the equilibrium shifts towards the bulk species and oxygen cannot accumulate in the near-surface region and therefore. On the other hand, accumulation of the oxygen species in the near surface region is critical to create a supersaturated solution, which is again required for triggering of critical PdO nucleation/phase formation. PdO nuclei on the 2D oxide phase were supposed to be catalytically active species in methane oxidation [34].

Our previous study [32] demonstrated that heating of Pd(111) in 0.4 mbar O_2 leads to the appearance of a specific surface 2D oxide at 655 K; this phase was also referred to as a Pd_5O_4 incommensurate surface oxide [9]. It is characterized by two $Pd3d_{5/2}$ peaks at 335.5 and 336.2 eV denoted as Pd_{ox1} and Pd_{ox2} along with the two O 1s peak at 528.9 and 529.6 eV denoted at O(I) and O(II) (for more details see Figure 1, Figure 2, and Table 1 in Ref. [32]). The Pd $3d_{5/2}$ peak at 336.6 eV due to the bulk PdO phase appeared at 720 K (for more detail see Figure 2, and Table 1 in Ref. [32]). Above 815 K the bulk PdO phase decomposed, leaving behind the dissolved oxygen species, which is characterized by the O 1s peak at 529.0 eV (see Figure 1 and Table 1 in Ref. [32]). The other interesting finding was that no PdO phase growth was observed during cooling [32]. The absence of the PdO phase, and the related strong temperature hysteresis of the oxidation kinetics, was explained by a combination of a lower concentration of the dissolved oxygen species in the near-surface region and a surface oxide different from Pd_5O_4 [32]. While Pd_5O_4 does

not form during cooling, supposedly the $\left(\sqrt{67} \times \sqrt{67}\right)R12.2°$ structure, forms [32]. This phase exhibits a lower oxygen density and is not favorable for PdO seeds to form.

In this paper we report on an *in-situ* investigation of *isothermal* oxidation of Pd(111) and Pd(110) in the mbar pressure range, with special focus on the time-resolved oxidation kinetics. Growth of the bulk PdO phase was confirmed from the PdO nuclei or "seeds" as it was supposed in Ref. [32]. The formation of the PdO seeds/particles adsorbed on the surface oxide was also supposed during the oxidation of Pd(111) by atomic oxygen [21]. As we discussed in our previous publication [32], PdO nucleation is facilitated by a combination of preferential oxygen dissolution in the near-surface region *(highest oxygen density below the surface)* with the optimum surface oxide precursor Pd_5O_4 *(highest oxygen density at the surface)*. A quasi-saturated oxygen solid solution should be achieved for the oxide phase to grow. It is conceivable that oxygen solubility, largely limited by the diffusion barrier through the surface lattice, should depend on the Pd surface density and therefore a close-packed surface such as Pd(111) should exhibit different oxidation kinetics than an open surface such as Pd(110). The heating ramp experiment, as in Refs. [32,33], might be not adequate to analyze the oxidation kinetics quantitatively. The rates of nucleation and growth should be both temperature/pressure dependent. In this paper, in order to study the oxidation kinetics separately as a function of pressure and temperature, isothermal experiments were performed, with a palladium single crystal being exposed to O_2 keeping temperature/pressure constant. Also, the presence of a surface-covering layer of 2D oxide could act as a "site-blocker" for oxygen adsorption from the gas phase, further slowing down the oxidation kinetics toward the 3D PdO phase. To verify these hypotheses, we followed oxidation of two palladium surfaces, (111) and (110), by ambient pressure XPS.

2. Experimental Methods

The experiments were performed at beamline U49/2-PGM2 at the synchrotron facility BESSY-2 in Berlin, Germany. The high-pressure XPS set-up, in detail described elsewhere [32,33], allowed us to acquire photoelectron spectra *in-situ* in the mbar pressure range. A sample was positioned inside an analysis chamber, which simultaneously serves as a high-pressure cell, 2 mm away from the aperture of 1 mm, used as an entrance to a differentially pumped electrostatic lens system and to a hemispherical analyzer (SPECS Scientific Instruments, Inc.). Temperature was measured by a chromel-alumel thermocouple (K-type) spot-welded onto the side of the sample. Heating of a sample was performed by an IR laser from the rear and the temperature was controlled with a thermal controller.

(111) and (110)-oriented Pd single crystals with orientation accuracy < 0.1° (both MaTecK GmbH) were used as samples. The cleaning procedures consisted of repeated cycles of Ar^+ sputtering at room and elevated temperatures, annealing at 950 K in UHV, and exposure to O_2 followed by flashing at 950 K for 60 seconds in UHV. In order to ensure reproducible initial conditions of the surface, the same standard cleaning cycle (Ar^+ sputtering and annealing at 950 K in UHV) was run before every experiment. The sample cleanness was checked by XPS.

The following experimental protocol was used to treat a sample in O_2. First, a sample was exposed to desired oxygen pressure at 350-400 K. Second, after oxygen pressure is stabilized, the sample was heated to a desired temperature with a typical heating rate of ~1.5 K/s. A low heating rate was used to avoid temperature oscillation. We did not detect any beam-induced oxidation/reduction during long-lasting experiments, which was tested by sample shifting to a new analysis spot.

The curve-fitting procedure is described in detail elsewhere (see for instance Ref. [33]). The line shape was assumed to be a Doniach-Sunjic function [35]. Both spin-orbital momentum peaks of the Pd 3d doublet were included in the fitting. Therefore, the Pd 3d spectra were fitted by three pairs of components for Pd 3d and one pair for plasmon excitation. The relative ratio of the peaks of the Pd 3d doublet was fixed during the fitting, whereas the other parameters such as intensity, FWHM and peak position were allowed to vary within a reasonable range.

3. Quantification of XPS Data

3.1. Calculation of oxide thickness

Oxide thickness can be calculated based on the approach proposed by Fadley [36]. For simplicity we assumed that oxide film, the 2D oxide or PdO, uniformly covers metallic palladium and that the 2D oxide and PdO has the same palladium atomic density, ρ_{PdO}, and the photoelectrons have the same Inelastic Mean Free Path (IMFP), Λ_e^{PdO}, in the 2D oxide and PdO. The intensity ratio between metallic component, $N_{Pd}(\theta)$, and the oxide component, $N_{ox}(\theta)$, can be used to calculate oxide layer thickness, t_{ox}, as shown below:

$$t_{ox} = \Lambda_e^{PdO} \times \ln\left(\frac{N_{ox}(\theta)}{N_{Pd}(\theta)} \frac{\rho_{Pd}}{\rho_{PdO}} \frac{\Lambda_e^{Pd}}{\Lambda_e^{PdO}} + 1 \right). \quad (1)$$

Here ρ_{Pd} and ρ_{PdO} are the palladium atomic densities of metallic palladium and palladium oxide, respectively, in atoms per cm^3; Λ_e^{Pd} and Λ_e^{PdO} are the IMFP for the Pd 3d photoelectron. The derivation of Eq.1 is given in the Supporting Information.

It should be underlined that IMFPs depend on the kinetic energy of the photoelectrons. For the photoelectron with the kinetic energy of 120 eV we used 0.417 and 0.465 nm for Pd metal and Pd oxides. It is not important for calculations using Eq.1 but we always normalize the intensities of the photoelectron peaks. The normalization was done on (a) the ring current, (b) the photon flux at a given photon energy. The relative sensitivity factors were also taken for proper photon energy [37].

3.2. Intensity variation of Pd $3p_{3/2}$ upon oxidation

The Pd $3p_{3/2}$ peak overlaps with the O 1s peak and this hinders quantitative and qualitative analysis, especially keeping in mind the Pd $3p_{3/2}$ and O 1s peaks shift upon oxidation. To make sure that our curve fitting protocol is valid and the Pd $3p_{3/2}$/O 1s region is representative, we have estimated the possible variation of the Pd $3d_{3/2}$ peak during transformation from the 2D oxide to the thick PdO layer. Two extreme cases were conceded: the 2D oxide and the "infinite" thick PdO layer. The 2D oxide is well characterized [9] and therefore can serve as a reference. The "infinite thick PdO layer" is assumed to have thickness greater than the information depth, which is approximately 1.5 nm for the photoelectrons with the kinetic energy of 120 eV (the photon energy of 650 eV).

Based on our XPS data and the calculations using Eq. 1, the thickness of the 2D oxide was estimated to be 0.52 nm. The Pd $3p_{3/2}$ emission consists of two contributions: from the 2D oxide and underlining palladium metal; these contributions cannot be separated. Apply Fadley's formalism [36] and assuming the intensity of the Pd $3p_{3/2}$ peak from the palladium metal substrate, $N_{Pd}(\theta)$ with the 2D oxide overlayer of thickness *t*, the ratio between the Pd $3p_{3/2}$ contributions for the 2D oxide and the "infinite thick PdO layer can be written as:

$$\frac{N_{\text{int}}^{tot}}{N_{fin}^{PdO}} = 1 - \left(1 - \frac{\rho_{Pd}\Lambda_e^{Pd}}{\rho_{PdO}\Lambda_e^{PdO}}\right)\exp\left(\frac{-t}{\Lambda_e^{PdO}}\right). \quad (2)$$

The detailed derivation is provided in the Supporting Information. Numerically the ratio was estimated to be 1.5. This value agrees with the number obtained from the curve fitting of the Pd $3p_{3/2}$/O 1s region. This was used as validation of the curve fitting protocol.

3. Results and Discussion

3.1. Pd(111)

The isothermal oxidation kinetics of palladium was studied on Pd(111) in 0.3 and 0.8 mbar O_2 at 650 K and 700 K and on Pd(110) in 0.2 and 0.6 mbar O_2 at 550 K and to 0.2 and 0.7 mbar O_2 at 575 K. The temperature ranges chosen for Pd(111) and Pd(110) were different due to oxidation kinetics as discussed below.

Figure 1 and Figure 2 show the evolution of the O 1s/Pd $3p_{3/2}$ and Pd 3d photoemission spectra of Pd(111) *in situ* as a function of time in 0.3 mbar O_2 at 650 K. To keep the same inelastic mean free pass (IMFP) of the photoelectrons emitted from the Pd 3d and O 1s/Pd $3p_{3/2}$ core levels, these two regions were collected at the photon energies of 460 and 650 eV, respectively, which resulted in the kinetic energy of the photoelectrons to be approximately 120 eV. It is critical to keep the same kinetic energy of the photoelectrons for all core levels of interest; otherwise, the photoelectrons traveling through the gas phase would experience the different attenuation and the quantification would be not straightforward. As shown in the right panel of Figure 1 and Figure 2, the O 1s/Pd $3p_{3/2}$ spectra were curve-fitted with four main components: O(I), O(II), O(III) and Pd $3p_{3/2}$; the Pd $3d_{5/2}$ spectra were fitted with three doublet components: Pd_{bulk}, Pd_{ox1} and Pd_{ox2} in the same way as in the Refs. [32,33]. The extra component for PdO was not added to the Pd 3d fitting; instead of this the Pd_{ox2} component was allowed to shift towards higher Binding Energies (BE). Therefore the Pd_{ox2} component was used to characterize both the 2D oxide and the bulk oxide phase. The O(II) component represents the 2D oxide and PdO, therefore the O(II) component was allowed to shift in the similar manner as in Ref. [31]. The BEs of the observed oxide species and their properties are summarized in Table 1. The Pd_{ox2}, O(II) and Pd $3p_{3/2}$ components were chosen to be representative of the degree of surface oxidation and the fractions of these components are plotted in Figure 3 for T = 700 K. The curves looks similar isothermal oxidation at T = 650 K (not shown here). The contribution of the Pd_{ox2} and O(II) components grew with time, whereas the Pd $3p_{3/2}$ component was losing intensity. Also the Pd $3p_{3/2}$ component was gradually shifting towards higher BEs due to palladium oxidation. The gas phase component of the O 1s peaks at about 538 eV was moving towards lower BEs because upon oxidation the volume charge of the gas phase changes. A lower density of palladium atoms in PdO comparing with metallic palladium can explain weakening of the Pd 3p3/2 component. The magnitude of change is in good agreement with our estimation (see Quantification of XPS Data Section). The expected decrease was estimated to be 1.5 times. The experimentally determined ratio between the initial intensity

and the final one, corresponding to the completely oxidized surface, varied between 1.5 and 2.2 (see for instance Figure 3). The experimental value is in a good agreement with the calculated value. This confirmed the appropriateness of our curve-fitting protocol and this means that the result curve-fitting can be used for quantitative analysis.

As one can see in Figure 3, the trends of the Pd_{ox2}, O(II) and Pd $3p_{3/2}$ components follow a S-shaped, or sigmoidal, profile pointing that the changes are slow in the beginning and then an acceleration is followed by slowing again. The latter slowing is due to a limited information depth: the oxide contribution saturates when the thickness of oxide reaches the information depth. For the kinetic energy of 120 eV, this number is approximately 2 nm. However, the initial slow reaction and the following acceleration are not artifacts and have been observed under all oxidation conditions. The slow initial oxidation, an induction period, lasts as long as 2.5 hours in 0.3 mbar O_2 at 700 K (Figure 3). From a spectroscopic point of view, no significant changes were observed in the spectra during the induction period: the Pd 3d and O 1s/Pd $3p_{3/2}$ spectra are similar to the fingerprints of the 2D oxide. However, a closer examination reveals that the ratios between Pd_{ox1} and Pd_{ox2} and between O(I) and O(II) slowly change. This can be explained by appearance of a "PdO-like" species and in our previous work it was assigned to the "PdO seeds" [32]. So the slow oxidation corresponds to formation of these PdO seeds or PdO nuclei. The Pd_{ox2} and O(II) components show the similar trend with the similar pivot points confirming indirectly correctness of our curve-fitting. On the other hand, the Pd_{ox2} component is more preferential for quantification of oxide film than O(II) because the O 1s/Pd $3p_{3/2}$ region is too complex and represents a few oxygen species. Keeping in mind the attenuation of the photoelectrons, oxide thickness (not the intensity) is likely the best representative of the oxidation kinetics. Oxide thickness was calculated using Eq. 1 based on the Pd 3d spectra and the results are plotted in Figure 4. The induction period is characterized oxide thickness of approximately 0.52 nm, which is close to the 2D oxide [9]. The oxide thickness grows rapidly after the induction period (Figure 4).

The duration of the induction period varies depending on the temperature and O_2 pressure: in 0.8 mbar O_2 it is ~ 45 min at 650 K and ~55 min at 700 K, whereas in 0.3 mbar O_2 it is ~80 min at 650 K and ~175 min at 700 K (Figure 4). At the higher pressure (0.8 mbar), the effect of temperature on the duration of the nucleation stage is not significant (see Figure 4). On the other hand at the low pressure (0.3 mbar), it increases more than twice as compared to the durations at 650 and 700 K indicated in Figure 4. Anyway the trend is clear: as oxygen pressure increases, the rate of oxidation rate increases as well, whereas with temperature the oxidation rate slows down. Likely this is a competition of two processes: formation of PdO nuclei of a certain size and their decomposition. The decomposition rate of the smaller PdO nuclei increases with temperature, whereas the likeliness of formation of larger nuclei is enhanced by increasing O_2 pressure due to larger supersaturation. A critical nucleus is generated by a statistical fluctuation once its radius exceeds a critical value

$$r_{critical} = \frac{2\gamma_s}{\Delta S \Delta T} \qquad (3)$$

.

Whereby the free energy gain by the bulk growth at a certain supersaturation (described in approximation by $\Delta S \Delta T$) of the nucleus just outbalances the free surface energy γ_S exhibiting the opposite sign. Consequently, both lower temperatures, i.e. a higher ΔT with respect to the PdO stability limit, and higher pressures mean higher supersaturation and enhance the statistical frequency of formation of critical nuclei. A limiting case is approached once oxygen pressure and temperature come close to the true thermodynamic stability limit of PdO: then the supersaturation becomes negligible and thus the critical nucleus size formally approaches infinity, meaning that the statistical probability to form such a nucleus approaches zero, and also the effective growth rate becomes zero.

Nucleus decomposition might also be enhanced through oxygen diffusion to the bulk, which is enhanced at higher temperatures. Oxygen diffusion into the palladium bulk results in depletion of oxygen concentration in the near-surface region and, therefore, sufficient oxygen supersaturation needed for fast oxide formation cannot be achieved [32]. On the other hand, the required oxygen population can be efficiently replenished at higher pressures; thus at 0.8 mbar O_2 the duration of the nucleation stage is almost the same at 650 K and at 700 K. After the induction period, the O(II) and PdO_{bulk} components grow quickly, which implies that the extended PdO phase growth is dominated by a sufficient number of already present stable nuclei. In Figure 4 one can see, the rate of the bulk PdO growth is dependent on O_2 pressure.

3.2. Pd(110)

The Pd(110) surface is more open in comparison with the close packed Pd(111) surface. Oxygen diffusion in the bulk should be facilitated on the open surface and therefore we expected easier (faster) oxidation on Pd(110). But the fast oxidation can occur only under conditions where a supersaturation of the nucleation-relevant near-surface regions with oxygen could be achieved. Surprisingly, a high temperature might be not the best condition due to unwanted fast diffusion into the deep bulk. In order to verify this, the same experimental protocol was used for both Pd(111) and Pd(110) surfaces: the single crystals were exposed to O_2 keeping the temperature and the pressure constant while the XPS spectra were acquired *in-situ*. First, Pd(110) was exposed to 0.2 mbar O_2 at 700 K and no trace of the PdO phase was detected even after 200 min treatment (spectra not shown here). On the other hand, in 0.7 mbar O_2 at 700 K Pd(110) was covered with the PdO phase within less than 30 min (spectra not shown here). This is much faster than oxidation of Pd(111) at the identical temperature and the pressure (see for instance Figure 4). The induction period could hardly be distinguished on Pd(110) under these conditions, meaning that the nucleation period was very short on Pd(110) in 0.7 mbar O_2 at 700 K. This observation is in a good agreement with the study by Westerstrom *et al.* [15] reported 'lack of surface oxide layers and facile bulk oxide formation on Pd(110)'. We think that these experiments demonstrated the importance of oxygen supersaturation in the near surface region for a high nucleation rate. Thus, at 0.2 mbar on the open Pd(110) surface, diffusion into the bulk is the dominating process, which successfully competes with accumulation of oxygen species in the near-surface region. Increasing the O_2 pressure to 0.7 mbar enhances the degree of oxygen supersaturation in the near surface region.

In order to suppress oxygen diffusion into the bulk, the sample temperature was decreased to 550 and 575 K. The examples of the O 1s/Pd $3p_{3/2}$ and Pd 3d core level spectra is shown in Figure 5 and Figure 6 obtained *in situ* from Pd(110) during oxidation in 0.2 mbar O_2 at 550 K. The O 1s/Pd $3p_{3/2}$ region was curve-fitted with four main components: O(I), O(II), O(III) and Pd $3p_{3/2}$ (Figure 5). The shape of the O 1s/Pd $3p_{3/2}$ peak is similar to the 2D Pd_5O_4 oxide on Pd(111) (for instance compare the spectrum for 19 min inFigure 5, with the spectrum for 40min in Figure 1), which means that on Pd(110) a specific surface oxide species (of yet unknown structure and exact stoichiometry) appears to be present and may also be beneficial to 3D PdO nucleation, just in analogy to Pd_5O_4 on Pd(111). From this analogy, the predicted difference between BEs of the O(I) and O(II) components should be 0.51 eV and the intensity ratio close to 1:1 (as for the 2D oxide on Pd(111) [9]), which is quite close to our observation on Pd(110). For Pd_5O_4 on Pd(111), the two oxygen components were assigned to two different oxygen coordination numbers with Pd. The Pd 3d spectrum obtained on Pd(110) after 25 min in 0.2 mbar O_2 (Figure 6) is similar to the 2D oxide spectrum on Pd(111) as well. Two oxygen-induced Pd $3d_{5/2}$ components, shifted towards higher BEs with respect to the metal peak, were reported for the 2D Pd_5O_4 oxide on Pd(111) (see for instance Figure 2, 37 min spectrum) [9,32,33]. Two different palladium components of the 2D oxide on Pd(111) correspond to two different coordination numbers of palladium atoms with oxygen. Again stressing the analogy with Pd(111), we suggest that the initial state of Pd(110) 0.2 mbar O_2 at 550 K, prior to 3D PdO nucleation, is also a 2D/Pd(110) surface oxide, which is also characterized by oxygen atoms in two different coordination positions and palladium atoms in two different coordination positions as well.

Similar to the Pd(111) case, the induction period is observed under all oxidation conditions. The duration of the induction period depend on the O_2 pressure and the temperature. At 575K in 0.7mbar, the induction period is hardly detectable, whereas at 550K in 0.2 and 0.6 mbar of O_2, the induction period is about 85 min. The oxide thickness grows rapidly after the induction period (**Figure 7**). Remarkable, the slope of the fast oxidation curves obtained at the same temperature is similar. On the one hand, this demonstrates that the reaction order of oxygen is zero. On the other hand slight temperature dependence agrees that the oxidation is an activated process. Oxygen diffusion to the bulk is suppressed at the low temperatures on Pd(110) and therefore diffusion does not compete with oxidation.

The nature of the species characterized by the O(III) component at 530.8 eV was not discussed. However, this component is clear distinguishable at later stage of the oxidation on Pd(111) and Pd(110) (see for instance Figure 1, spectrum for 249 min and Figure 5, spectrum for 197 min). The intensity of the O(III) component was growing with PdO and the depth profiling varying the photon energy demonstrated the surface nature of this species. We supposed that the O(III) component is characteristic of PdO_2.

3.3. Comparing Pd(111) and (110) surfaces

A few differences between the Pd(111) and Pd(110) surfaces can be noticed (1) the oxidation temperature is more than 100 degrees lower for Pd(110), and (2) typically the duration of the nucleation period is shorter for Pd(110). The other remarkable difference can be seen comparing **Figure 4** and **Figure 7**: the oxidation rate (during the second stage – the fast oxidation) is a temperature independent but a pressure dependent on Pd(111) (**Figure 4**) whereas on

Pt(110) the oxidation rate is visa versa: temperature dependent and a pressure independent (**Figure 7**). Switching between Pd(111) and Pd(110) results in that the oxidation regime changes.

The first stage of palladium oxidation, the induction period, is associated with appearance of PdO nuclei. The oxide phase forms based on the PdO nuclei and the time required for the transformation is a function of temperature/pressure. At the low temperatures, the phase growth requires longer time because the transport (diffusion) processes required for the formation of critical nuclei are kinetically limited. At higher temperatures, the process slows due to thermodynamic limitations. These considerations can be used to explain qualitatively the difference in the pressure and temperature trends of oxidation of Pd(111) and Pd(110). Oxidation of Pd(111) was performed at 650 and 700 K. Likely, these temperatures are already close to the thermodynamic stability limit of PdO and the process there is thermodynamically controlled PdO nucleation. Pd(110) was oxidized at 550 and 575 K. At these temperatures nucleation/oxidation is predominantly kinetically controlled.

At the second stage, the oxidation rate is independent on the temperature on Pd(111); the slope of the oxide thickness is approximately the same at 650 and 700K. However, the oxidation rate increases with the pressure, which might be an effect of the diffusion of oxygen in the bulk. At high temperatures, the diffusion rate becomes essential and diffusion competes with oxidation. This was clear for the open surface, Pd(110), when palladium could not be oxidized in 0.2 mbar O_2 at 700 K due to the fast oxygen diffusion in the bulk on the open surface. The oxygen supersaturation in the near-surface region was achieved and the surface was oxidized very fast in 0.7 mbar O_2. At the lower temperature (550 and 575K), the diffusion is not essential and, as a result, no pressure dependence is observed (Figure 7).

Summary

Oxidation of the Pd(111) and Pd(110) surfaces was studied by ambient pressure XPS in the mbar range of O_2 at $550<T<700$ K. It was found that oxidation is slow in the beginning on both surfaces and then accelerates. The initial slow oxidation, the induction period, is governed by nucleation of PdO "seeds". Pd(110) could be oxidized at lower temperatures than Pd(111) at the same O_2 pressure. Due to the higher temperature, on Pd(111) the statistical rate of formation of critical nuclei is thermodynamically limited, therefore a temperature increase causes the requirement of larger critical nuclei and thus lowers the frequency of nucleus formation over time and thus also the overall rate of oxidation. Oxidation of Pd(110) runs at lower temperature and therefore nucleus formation is kinetically limited. Low temperature oxidation of Pd(110) was possible because the open Pd(110) surface has a higher oxygen permeability and a supersaturated oxygen concentration in the near surface region can be achieved more easily. Depth profiling varying photon energy demonstrated that oxidation propagates in the bulk of palladium and along the surface. Likely, the PdO_2 species exists on the surface of PdO.

Acknowledgement

This project was supported through EU program RII3-CT-2004-506008 (proposal No. 2007_1_60973; User Project Acronym: BESSY-ID.07.1.973). The authors thank the BESSY staff for their support of the in situ XPS measurements. Support from the Department of Energy, Office of Basic Energy Sciences, under grant DE-FG02-03ER15408 is gratefully acknowledged.

Table 1 Photoemission characteristics of the different oxide species reported in Refs.[32,33]

Species	Conditions	O 1s, eV	Pd $3d_{5/2}$, eV	Comments
Pd_5O_4, surface 2D oxide	Heating in 0.4 mbar O_2, at 655 K	528.9 and 529.6	335.5 and 336.2	Two BEs corresponds two types of oxygen/palladium coordination;[9] Decomposes at ~ 800 K
bulk PdO phase	Heating in 0.4 mbar O_2, at 720 K	529.7	336.6	Appears at 655 K Decomposes at 815 K
Dissolved oxygen atoms	Heating 0.4 mbar O_2, above 815 K	529.0	-	Desorbs above 1070 K
$(\sqrt{67} \times \sqrt{67})R12.2°$	Cooling in 0.4 mbar O_2	528.9 and 529.6	335.4 and 336.6	Two BEs corresponds two types of oxygen/palladium coordination[9]

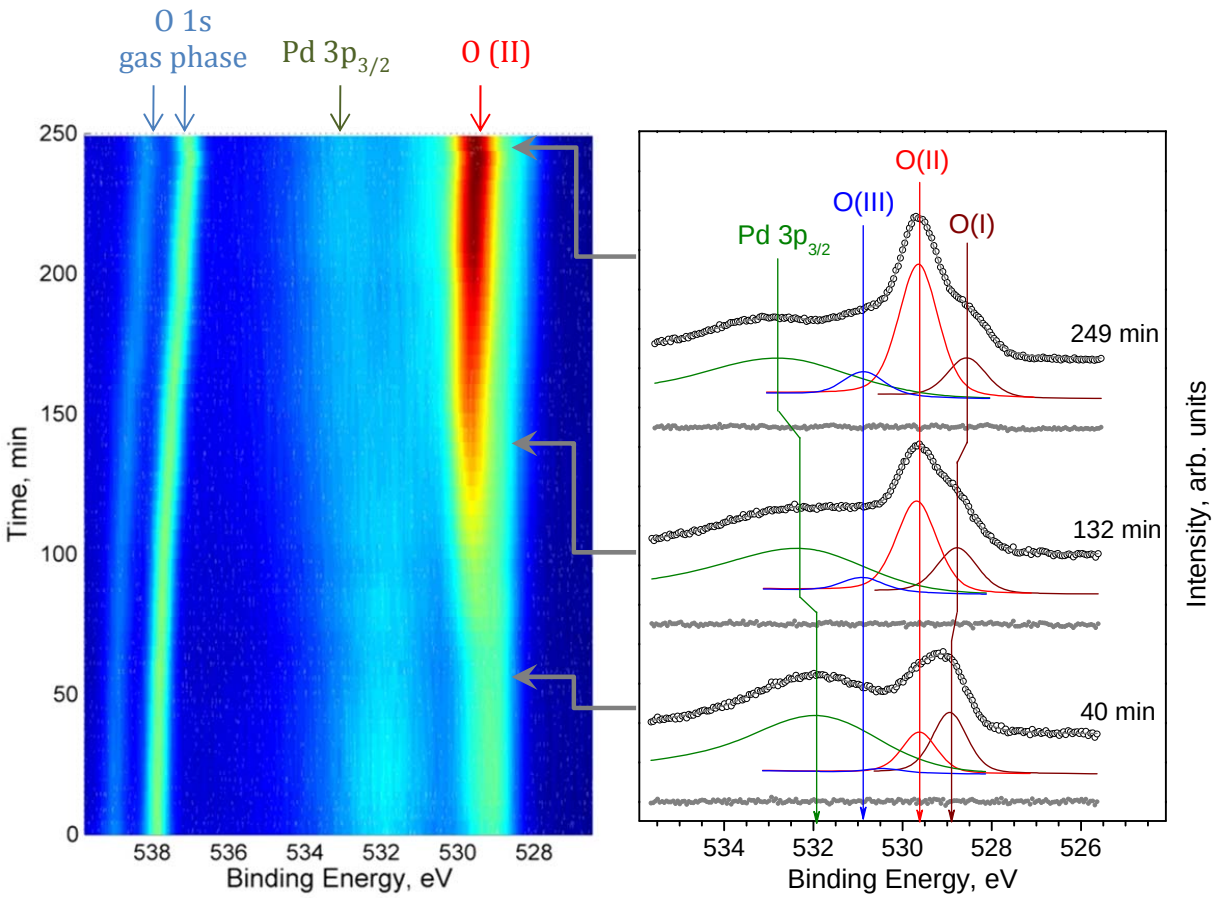

Figure 1 The O 1s/Pd $3p_{3/2}$ photoemission spectra obtained *in situ* from Pd(111) as a function of time in 0.3 mbar O_2 at 650K. Photon energy is 650 eV. Open circles are raw data. The gray dots under each spectrum represent misfitting. (Color *on-line*)

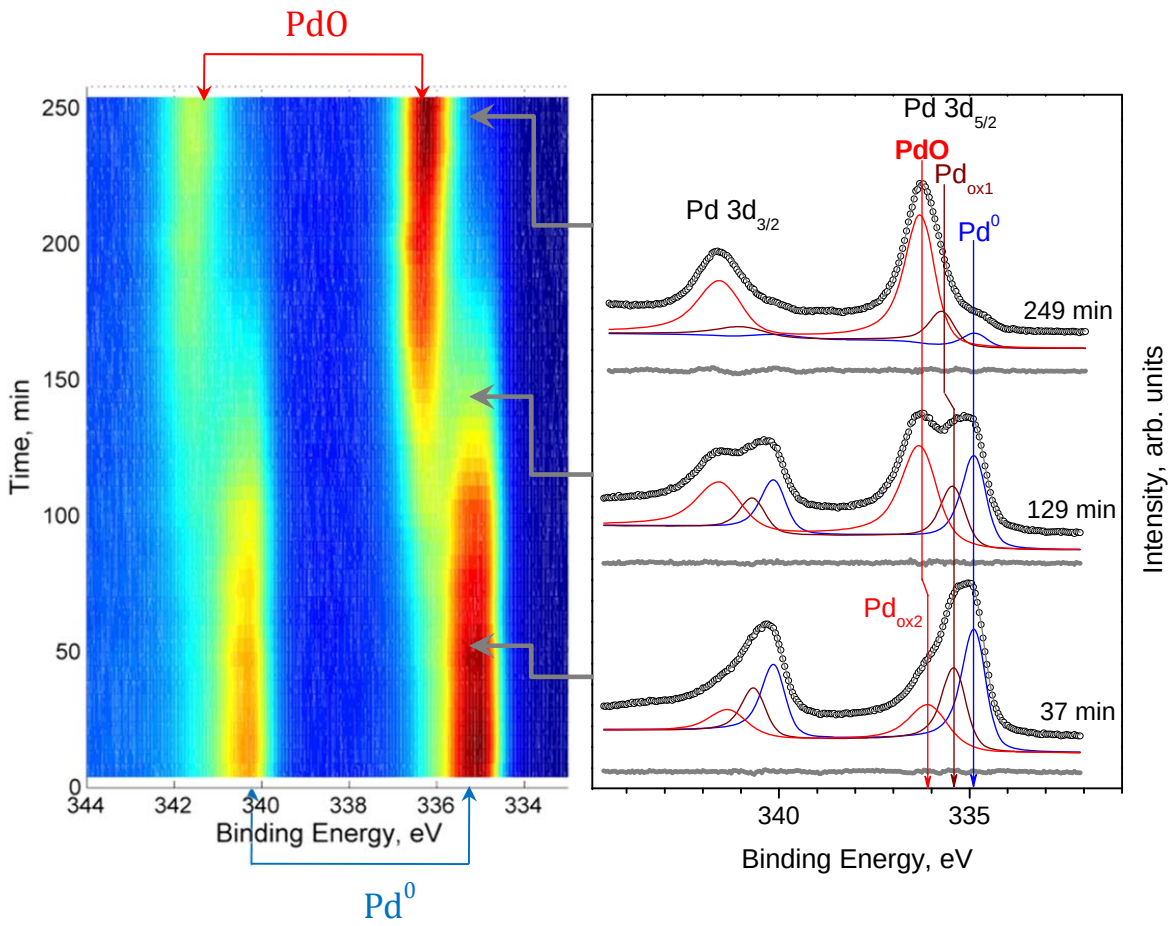

Figure 2 The Pd $3d_{5/2}$ photoemission spectra obtained *in situ* from Pd(111) as a function of time in 0.3 mbar O_2 at 650K. Photon energy is 460 eV. Open circles are raw data. The gray dots under each spectrum represent misfitting. (Color *on-line*)

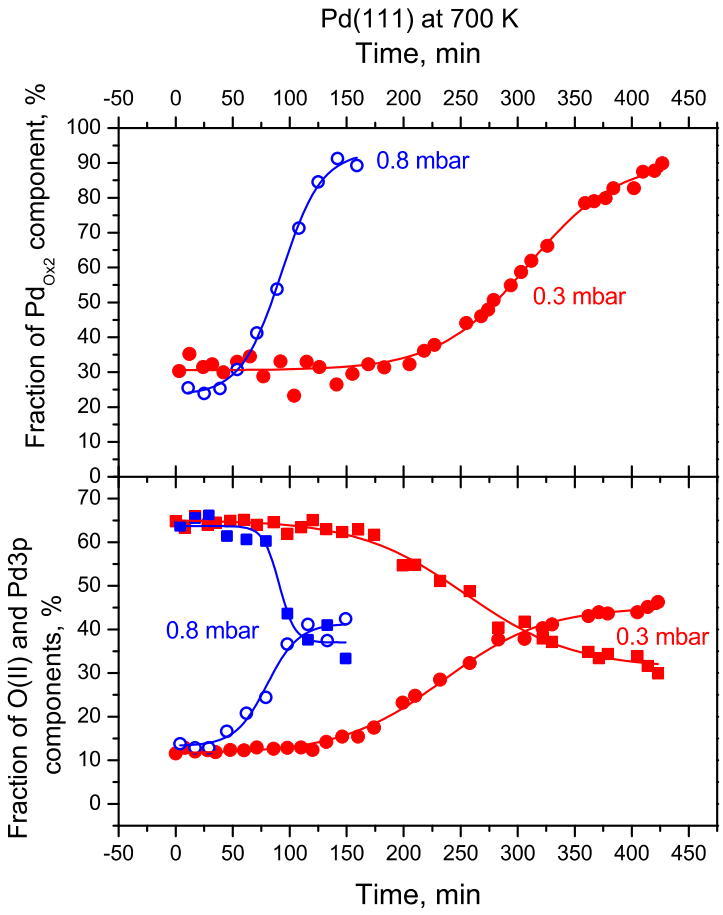

Figure 3 Pd(111): fraction of O(II) (circles) and Pd 3p (squares) components (the bottom panel) along with the Pd_{Ox2} component (the top panel) as a function of time at 700 K in 0.3 (filled) and 0.8 mbar O_2 (open). Sigmoidal curve-fitting shown is provided to improve the visibility of the trends. (Color *on-line*)

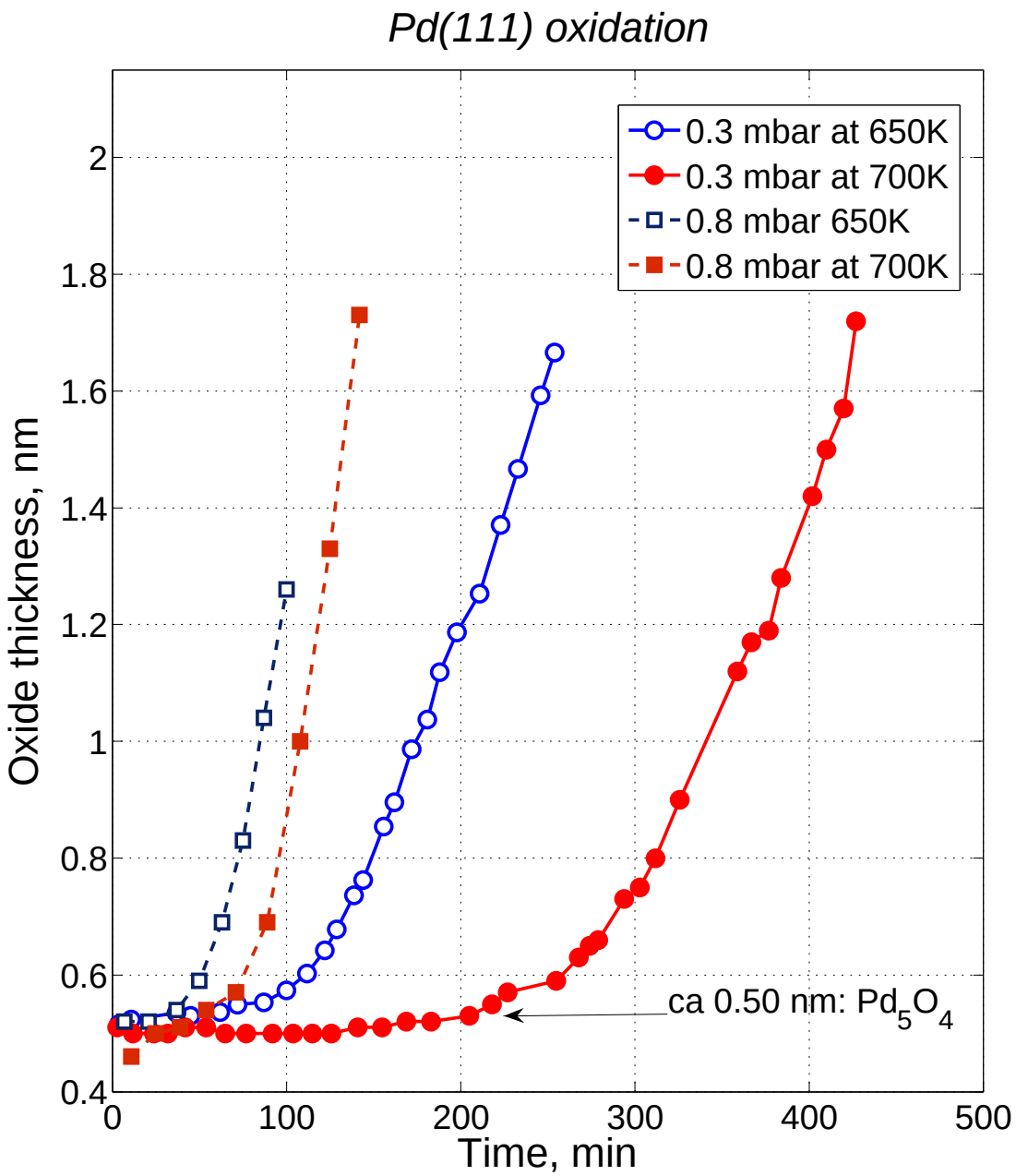

Figure 4 Oxide thickness on Pd(111) as a function of time: open markers are for oxidation at 650K and the filled markers are for at 700K; the circles are for 0.3 mbar and squares are for 0.8 mbar. The thickness was calculated using Eq. 1 based on the Pd 3d spectra. (Color *on-line*)

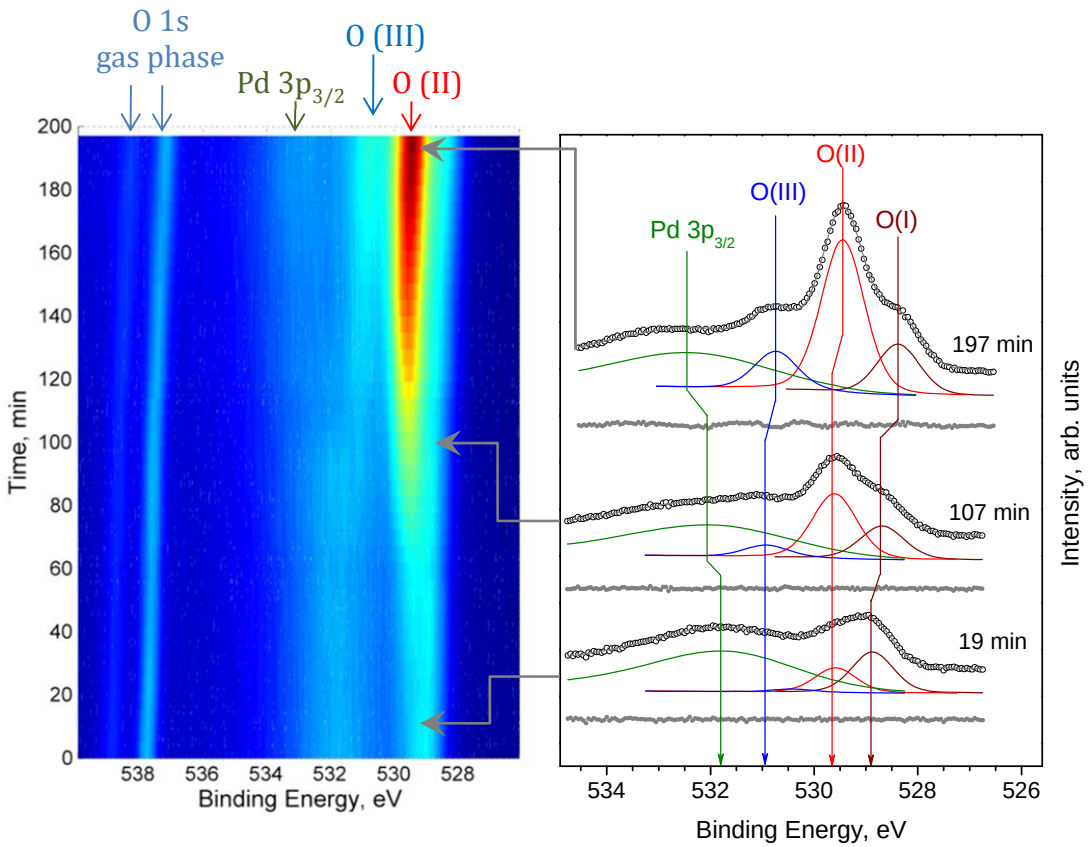

Figure 5 The O 1s/Pd $3p_{3/2}$ photoemission spectra obtained *in situ* from Pd(110) as a function of time in 0.224 mbar O_2 at 550K. Photon energy is 650 eV. Open circles are raw data. The gray dots under each spectrum represent misfitting. (Color *on-line*)

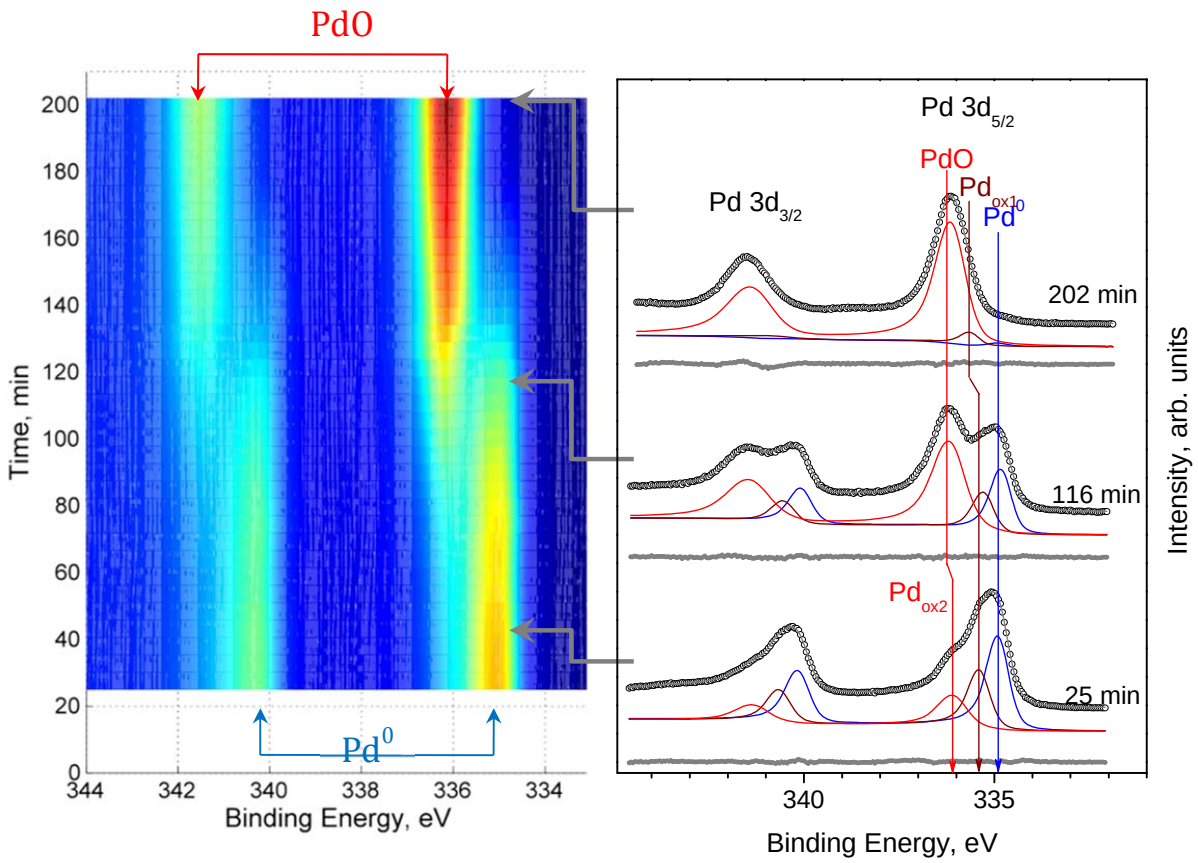

Figure 6 The Pd $3d_{5/2}$ photoemission spectra obtained *in situ* from Pd(110) as a function of time in 0.224 mbar O_2 at 550K. Photon energy is 460 eV. Open circles are raw data. The gray dots under each spectrum represent misfitting. (Color *on-line*)

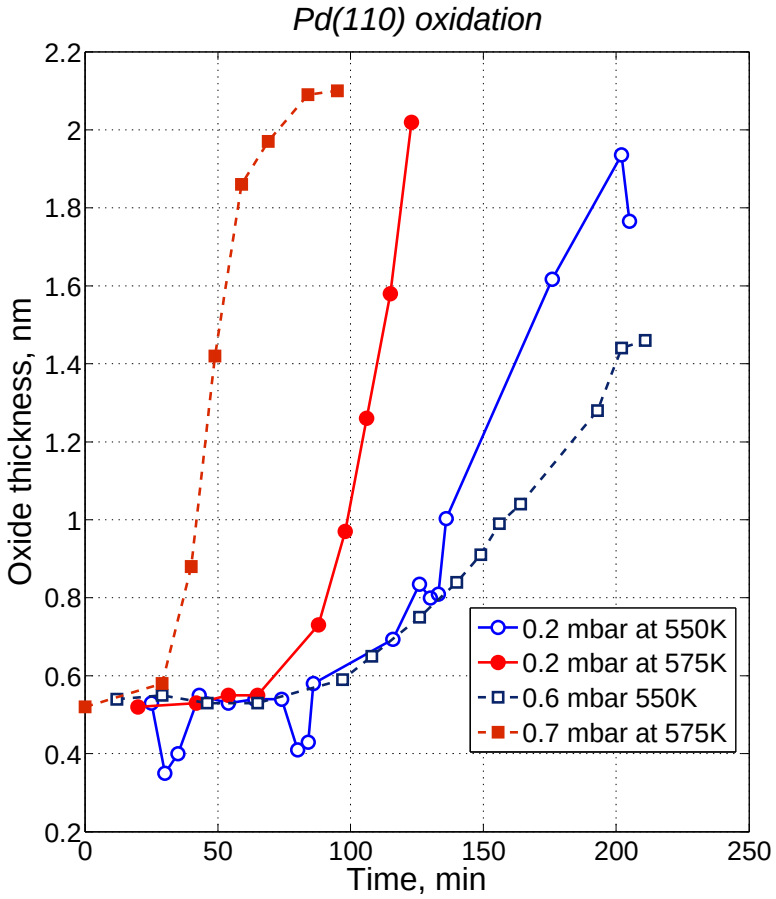

Figure 7 Oxide thickness on Pd(110) as a function of time: open markers are for oxidation at 550K and the filled markers are for at 575K; the circles are for 0.2 mbar and squares are for 0.6 and 0.7 mbar. The thickness was calculated using Eq. 1 based on the Pd 3d spectra. (Color *on-line*)

References

1. Bondzie VA, Kleban PH, Dwyer DJ (2000) Kinetics of PdO formation and CO reduction on Pd(110). Surf Sci 465 (3):266-276

2. Monteiro RS, Zemlyanov D, Storey JM, Ribeiro FH (2001) Surface area increase on Pd foils after oxidation in excess methane. J Catal 201 (1):37-45

3. Monteiro RS, Zemlyanov D, Storey JM, Ribeiro FH (2001) Turnover Rate and Reaction Orders for the Complete Oxidation of Methane on a Palladium Foil in Excess Dioxygen. J Catal 199 (2):291-301

4. Zheng G, Altman EI (2002) The Reactivity of Surface Oxygen Phases on Pd(100) Toward Reduction by CO. J Phys Chem B 106 (5):1048-1057

5. Altman EI (2003) The reaction of propene with oxygen-covered Pd(1 0 0). Surf Sci 547 (1-2):108-126

6. Zhu G, Han J, Zemlyanov DY, Ribeiro FH (2005) Temperature Dependence of the Kinetics for the Complete Oxidation of Methane on Palladium and Palladium Oxide. J Phys Chem B 109 (6):2331-2337

7. Gabasch H, Kleimenov E, Teschner D, Zafeiratos S, Havecker M, Knop-Gericke A, Schlogl R, Zemlyanov D, Aszalos-Kiss B, Hayek K, Klotzer B (2006) Carbon incorporation during ethene oxidation on Pd(111) studied by in situ X-ray photoelectron spectroscopy at 2 x 10-3 mbar. J Catal 242 (2):340-348

8. Warner JS (1967) The free energy of formation of palladium oxide. J Electrochem Soc 114 (1):68-71

9. Lundgren E, Kresse G, Klein C, Borg M, Andersen JN, De Santis M, Gauthier Y, Konvicka C, Schmid M, Varga P (2002) Two-dimensional oxide on Pd(111). Phys Rev Lett 88 (24):246103/246101-246103/246104

10. Zheng G, Altman EI (2000) The oxidation of Pd(111). Surf Sci 462 (1-3):151-168

11. Conrad H, Ertl G, Kueppers J, Latta EE (1977) Interaction of nitric oxide and oxygen with palladium(111) surfaces. I. Surf Sci 65 (1):235-244

12. Campbell CT, Foyt DC, White JM (1977) Oxygen penetration into the bulk of palladium. J Phys Chem 81 (5):491-494

13. Weissman DL, Shek ML, Spicer WE (1980) Photoemission spectra and thermal desorption characteristics of two states of oxygen on palladium. Surf Sci 92 (2-3):L59-L66

14. Leisenberger FP, Koller G, Sock M, Surnev S, Ramsey MG, Netzer FP, Klotzer B, Hayek K (2000) Surface and subsurface oxygen on Pd(111). Surf Sci 445 (2-3):380-393

15. Westerstrom R, Weststrate CJ, Gustafson J, Mikkelsen A, Schnadt J, Andersen JN, Lundgren E, Seriani N, Mittendorfer F, Kresse G, Stierle A (2009) Lack of surface oxide layers and facile bulk oxide formation on Pd(110). Phys Rev B: Condens Matter Mater Phys 80 (12):125431/125431-125431/125411

16. Westerstroem R, Weststrate CJ, Resta A, Mikkelsen A, Schnadt J, Andersen JN, Lundgren E, Schmid M, Seriani N, Harl J, Mittendorfer F, Kresse G (2008) Stressing Pd atoms. Initial oxidation of the Pd(110) surface. Surf Sci 602 (14):2440-2447

17. Kostelnik P, Seriani N, Kresse G, Mikkelsen A, Lundgren E, Blum V, Sikola T, Varga P, Schmid M (2007) The Pd(100)-(.sqroot..hivin.5 Ã— .sqroot..hivin.5)R27Â°-O surface oxide: A LEED, DFT and STM study. Surf Sci 601 (6):1574-1581

18. Zheng G, Altman EI (2002) The oxidation mechanism of Pd(100). Surf Sci 504 (1-3):253-270

19. Westerstrom R, Gustafson J, Resta A, Mikkelsen A, Andersen JN, Lundgren E, Seriani N, Mittendorfer F, Schmid M, Klikovits J, Varga P, Ackermann MD, Frenken JWM, Kasper N, Stierle A (2007) Oxidation of Pd(553): From ultrahigh vacuum to atmospheric pressure. Phys Rev B: Condens Matter Mater Phys 76 (15):155410/155411-155410/155419

20. Klikovits J, Napetschnig E, Schmid M, Seriani N, Dubay O, Kresse G, Varga P (2007) Surface oxides on Pd(111): STM and density functional calculations. Phys Rev B: Condens Matter Mater Phys 76 (4):045405/045401-045405/045409

21. Kan HH, Weaver JF (2009) Mechanism of PdO thin film formation during the oxidation of Pd(111). Surf Sci 603 (17):2671-2682

22. Kan HH, Weaver JF (2008) A PdO(1 0 1) thin film grown on Pd(1 1 1) in ultrahigh vacuum. Surf Sci 602 (9):L53-L57

23. Kan HH, Shumbera RB, Weaver JF (2008) Adsorption and abstraction of oxygen atoms on Pd(111): Characterization of the precursor to PdO formation. Surf Sci 602 (7):1337-1346

24. Altman EI (2009) On the mechanism of the transition from surface to bulk metal oxides (A perspective on the article "Mechanism of PdO thin film formation during the oxidation of Pd(111)"). Surf Sci 603 (17):2669-2670

25. Wang J, Yun Y, Altman EI (2007) The plasma oxidation of Pd(1 0 0). Surf Sci 601 (16):3497-3505

26. Yudanov IV, Neyman KM, Rosch N (2004). Physical Chemestry and Chemical Physics 6:116-123

27. Han J, Zemlyanov DY, Ribeiro FH (2006) Interaction of O2 with Pd single crystals in the range 1-150 Torr. Oxygen dissolution and reaction. Surf Sci 600 (13):2752-2761

28. Han J, Zemlyanov DY, Ribeiro FH (2006) Interaction of O2 with Pd single crystals in the range 1-150 Torr. Surface morphology transformations. Surf Sci

600 (13):2730-2744

29. Pantfoeder J, Poelmann S, Zhu JF, Borgmann D, Denecke R, Steinruek HP (2005) New setup for in situ x-ray photoelectron spectroscopy from ultrahigh vacuum to 1 mbar. Rev Sci Instrum 76 (1):014102/014101-014102/014109

30. Salmeron M, Schlogl R (2008) Ambient pressure photoelectron spectroscopy. A new tool for surface science and nanotechnology. Surf Sci Rep 63 (4):169-199

31. Ketteler G, Ogletree DF, Bluhm H, Liu H, Hebenstreit ELD, Salmeron M (2005) In Situ Spectroscopic Study of the Oxidation and Reduction of Pd(111). J Am Chem Soc 127 (51):18269-18273

32. Gabasch H, Unterberger W, Hayek K, Kloetzer B, Kleimenov E, Teschner D, Zafeiratos S, Haevecker M, Knop-Gericke A, Schloegl R, Han J, Ribeiro FH, Aszalos-Kiss B, Curtin T, Zemlyanov D (2006) In situ XPS study of Pd(1 1 1) oxidation at elevated pressure, Part 2: Palladium oxidation in the 10-1 mbar range. Surf Sci 600 (15):2980-2989

33. Zemlyanov D, Aszalos-Kiss B, Kleimenov E, Teschner D, Zafeiratos S, Haevecker M, Knop-Gericke A, Schloegl R, Gabasch H, Unterberger W, Hayek K, Kloetzer B (2006) In situ XPS study of Pd(111) oxidation. Part 1: 2D oxide formation in 10-3 mbar O2. Surf Sci 600 (5):983-994

34. Gabasch H, Hayek K, Kloetzer B, Unterberger W, Kleimenov E, Teschner D, Zafeiratos S, Haevecker M, Knop-Gericke A, Schloegl R, Aszalos-Kiss B, Zemlyanov D (2007) Methane Oxidation on Pd(111): In Situ XPS Identification of Active Phase. J Phys Chem C 111 (22):7957-7962

35. Doniach S, Sunjic M (1970). J Phys Chem C 31:285

36. Fadley CS (1978) Basic concepts of x-ray photoelectron spectroscopy. Electron Spectrosc: Theory, Tech Appl 2:1-156

37. Yeh JJ, Lindau I (1985) Atomic subshell photoionization cross sections and asymmetry parameters: $1 \leq Z \leq 103$. At Data Nucl Data Tables 32 (1):1-155. doi:10.1016/0092-640x(85)90016-6